

Using Building Integrated Photovoltaic Thermal (BIPV/T) Systems to Achieve Net Zero Goal: Current Trends and Future Perspectives



Ali Sohani, Cristina Cornaro, Mohammad Hassan Shahverdian, Saman Samiezadeh, Siamak Hoseinzadeh, Alireza Dehghani-Sanij, Marco Pierro, and David Moser

Introduction

According to some estimates, by 2035, the global energy consumption rate will have undergone a 50% rise from 1990 levels. This predicted rise will stem from large increases in population growth and urbanization and will influence the energy consumption of buildings. Today, buildings account for 40% of global energy consumption [1–3], with nonrenewable energy being consumed for their cooling, heating, and lighting [4].

In large cities, for instance, Tokyo, San Francisco, Hong Kong, and New York, buildings account for significantly greater greenhouse gas (GHG) emission and energy consumption than transportation does [5]. In response, global roadmaps are

A. Sohani · C. Cornaro

Department of Enterprise Engineering, University of Rome Tor Vergata, Rome, Italy
e-mail: ali.sohani@uniroma2.it; cornaro@uniroma2.it

M. H. Shahverdian · S. Samiezadeh

Optimization of Energy Systems' Installations Lab., Faculty of Mechanical Engineering-Energy Division, K.N. Toosi University of Technology, Tehran, Iran

S. Hoseinzadeh

Department of Planning, Design, and Technology of Architecture, Sapienza University of Rome, Rome, Italy

e-mail: siamak.hosseinzadeh@uniroma1.it

A. Dehghani-Sanij (✉)

Waterloo Institute for Sustainable Energy (WISE), University of Waterloo,
Waterloo, ON, Canada

e-mail: a7degha@uwaterloo.ca; alireza.dehghanisanij@uwaterloo.ca; ads485@mun.ca

M. Pierro · D. Moser

EURAC Research, Bolzano, Italy

e-mail: marco.pierro@eurac.edu; david.moser@eurac.edu

© The Author(s), under exclusive license to Springer Nature

Switzerland AG 2023

A. Sayigh (ed.), *Towards Net Zero Carbon Emissions in the Building Industry*,
Innovative Renewable Energy, https://doi.org/10.1007/978-3-031-15218-4_5

seeking to replace the fossil fuels used to power buildings with renewable, clean energy resources, with the goal of changing buildings with high energy consumption into net zero energy ones [6, 7]. Therefore, decarbonization has become a great environmental priority, and new buildings designed to be net zero are a focus in the European Union (EU). The UK is hoping to achieve an 80% decline in national emissions by 2050 and then to modify the plan for zero emission systems [8]. Japan intends for its public and residential buildings to be net zero energy buildings (NZEBs) by 2020 and 2030, respectively [9]. Furthermore, after 2030, new US commercial buildings will be required to be net zero. Meeting these goals will require the reduction of primary building energy consumption through energy-efficient envelopes [10].

Photovoltaic (PV) systems are a promising alternative for harnessing clean, inexhaustible, and abundant solar power for the generation of environmentally benign energy [11]. In Italy, attempts are being made to achieve the goal of using 55% renewable energy resources for the country's power supply. The power production of PV technologies is planned to increase from 25 TWh per year at the present time to 72 TWh per year in 2030 [12]. Moreover, German PV installations have reached a total energy capacity of 50 GW and are expected to generate up to 413 GW by 2050 [13]. The global market for PV solutions is also expected to enjoy a 1.7% growth per year, suggesting a rise from approximately 42,000 million USD in 2019 to around 47,000 million USD in 2024 [14]. The permanent load of a building, including concrete rooftops and walls, can be replaced with PV systems, leading to fossil energy-free buildings and a pollution-free environment [14].

Building integrated photovoltaics (BIPVs) are solar-generating components that can be used to replace traditional construction materials and envelopes (e.g., shading, atria, window, and roof components) with PV and so support clean power generation. Hence, BIPV provides a building envelope and supplies electricity. New buildings can be constructed using BIPV, and existing buildings can have it retrofitted. In light of its dual functionality, BIPV is an efficient and effective approach to decreasing construction labor and material costs. In addition, BIPV helps maintain the decorative features of buildings. Thus, the implementation of BIPV has grown significantly in recent years. Semitransparent BIPV structures (e.g., glass-on-glass) have become an appealing choice for architects as they can provide an excellent exterior appearance while allowing daylight into buildings and controlling solar gain. They are also appealing for facade glazing [15]. In a BIPV, the system produces electricity, while no heat from the panel is recovered. When there is heat recovery from the panel, the system is called BIPV/T [16]. BIPV/T technologies have better energy efficiency in comparison to BIPV systems. Furthermore, due to saving more fossil fuels, they enjoy the better environmental performance as well [17].

Having briefly introduced BIPV/T systems, this chapter next discusses their working principles, their use in different parts of a building, and mathematical modeling of BIPV/T units in both free and forced convection conditions. The net zero goal is described as is the role of BIPV/T systems in reaching this goal.

BIPV/T Systems: How They Work

A BIPV/T system is schematically depicted in Fig. 1. In such a system, on the one hand, a portion of the radiation gained from the sun by PV supports electricity generation. On the other hand, air flows through the channel between the PV and building wall and absorbs a part of the irradiance that is not transformed into electricity. The inlet air can be totally supplied from the atmosphere, or it be a mixture of rooms' return air and ambient air. The outlet air can also be utilized for space heating in cold seasons and desiccant regeneration in hot seasons. These options mean energy, and consequently money, is saved, and fossil fuels need not be consumed for space heating or desiccant regeneration, so GHG emissions are negligible [18].

In addition to installation on the sidewalls of buildings, BIPV/T systems can be installed on roofs [19]. Over time, BIPV/T systems have gradually come to be used in other parts of buildings as well. In fact, it is now possible to use these systems in all parts of buildings' exterior shells, such as roofs, facades, walls, skylights, or special structures such as ledges and awnings [16]. Therefore, it is not too unlikely that BIPV/T systems will soon reach cover the entire exterior of the buildings and can be designed to be architecturally attractive as well as functional [20]. Moreover, PV cells can be employed in the form of dye-sensitized solar cells, offering the opportunity of using them in windows [21].

Mathematical Modeling

This section focuses on system modeling. A BIPV/T system, in addition to the air duct behind the panels, consists of five layers: glass, top EVA (ethylene vinyl acetate), silicon, bottom EVA, and Tedlar, which are further modeled. The sketch of

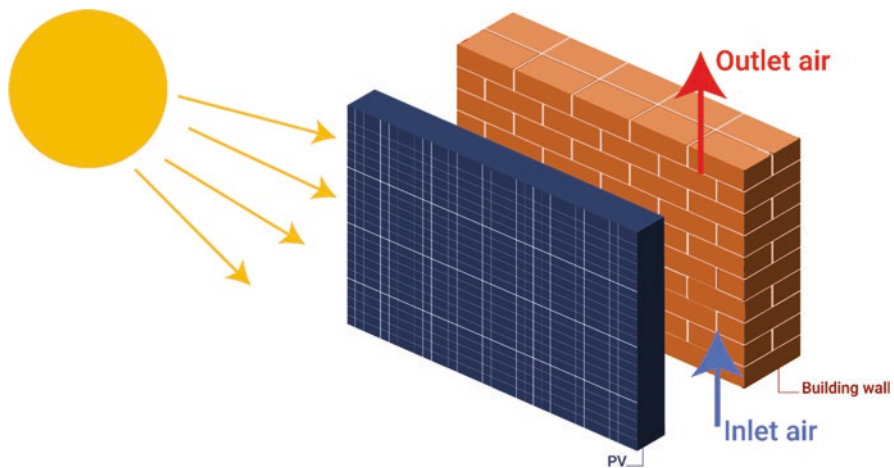


Fig. 1 Working principle of a building integrated photovoltaic thermal (BIPV/T) system [17]

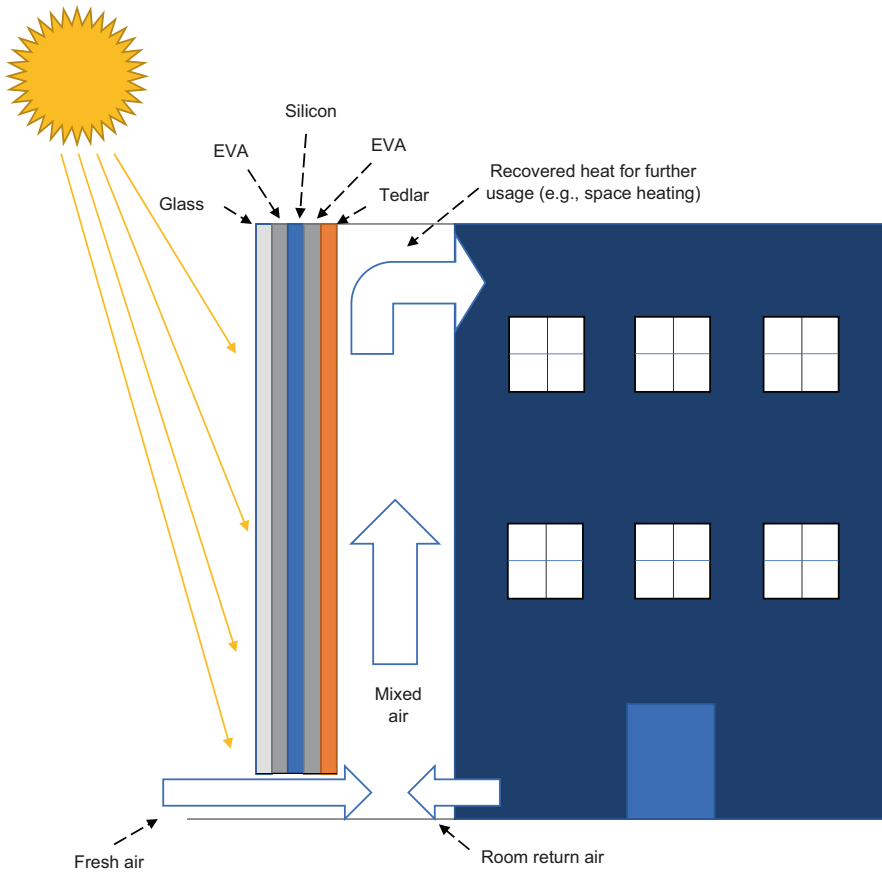


Fig. 2 The sketch of BIPV/T system considered for modeling by the explained approach in part 3

BIPV/T system considered for modeling by the explained approach is illustrated in Fig. 2.

Glass

Energy enters the glass layer through the transfer of conductive heat between the top layer of EVA and the glass as well as the sun’s radiation. The energy output of the glass layer is through heat transfer and radiation between the glass and the ambient air, as seen in Eq. (1):

$$c_{p,g} \delta_g A \rho_g \frac{dT_g}{dt} = \alpha_g GA + Q_{\text{cond-EVA1,g}} - Q_{\text{conv-g,a}} - Q_{\text{rad-g,sky}} \tag{1}$$

where the subtitle *g* symbolizes glass, *a* is the ambient air, and c_p , δ , A , ρ , T , t , α , G , Q_{cond} , Q_{conv} , and Q_{rad} represent the specific heat capacity, thickness, area, density, temperature, time, absorption coefficient, solar radiation, conductive heat transfer, convective heat transfer, and radiant heat transfer, respectively.

In Eq. (1), the terms from the left are:

- Glass energy changes
- Heat absorbed by receiving solar radiation
- Conductive heat transfer between the glass layer and the top layer of EVA
- Convective heat transfer between the glass layer and the ambient air
- Radiation from glass to the sky

The coefficient of conductive heat transfer is calculated from Eq. (2):

$$Q_{\text{cond-EVA1,g}} = \frac{T_{\text{EVA1}} - T_{\text{g}}}{R_{\text{EVA1,g}}} \quad (2)$$

where $R_{\text{EVA1,g}}$ is the thermal resistance between the glass and EVA layers and can be calculated from Eq. (3):

$$R_{\text{EVA1,g}} = \frac{\delta_{\text{EVA1}}}{2k_{\text{EVA1}}A_{\text{EVA1}}} + \frac{\delta_{\text{g}}}{2k_{\text{g}}A_{\text{g}}} \quad (3)$$

where thermal conductivity is shown by k .

The convective heat transfer between the glass layer and the ambient air is obtained from Eq. (4):

$$Q_{\text{conv-g,a}} = \frac{T_{\text{g}} - T_{\text{a}}}{R_{\text{conv-g,a}}} \quad (4)$$

where the thermal resistance and convective heat transfer coefficient are obtained from Eqs. (5) and (6) [22]:

$$R_{\text{conv-g,a}} = \frac{1}{h_{\text{conv-g,a}}A} \quad (5)$$

$$h_{\text{conv-g,a}} = 2.8 + 3U \quad (6)$$

The wind speed is shown by U .

The relationship in the radiant heat transfer between the glass layer and the sky is as follows:

$$Q_{\text{rad-g,sky}} = \frac{T_{\text{g}} - T_{\text{sky}}}{R_{\text{rad-g,sky}}} \quad (7)$$

Thermal resistance and the sky temperature can be calculated by Eqs. (8) and (9) [23]:

$$R_{\text{rad-g,sky}} = \frac{1}{\sigma \varepsilon_g A (T_g^2 + T_{\text{sky}}^2) (T_g + T_{\text{sky}})} \quad (8)$$

$$T_{\text{sky}} = 0.0552 T_a^{1.5} \quad (9)$$

In Eq. (8), σ is the Stefan-Boltzmann coefficient, and ε is the emission coefficient.

Top EVA

The input energy arrives at the top EVA layer through conduction between the top EVA and silicon; output energy from the top EVA layer is through the conduction heat transfer between the EVA and glass layers, as shown in Eq. (10). In the following relations, the PV caption symbolizes the silicon layer.

$$c_{p,EVA1} \delta_{EVA1} A \rho_{EVA1} \frac{dT_{EVA1}}{dt} = Q_{\text{cond-PV,EVA1}} - Q_{\text{cond-EVA1,g}} \quad (10)$$

In Eq. (10), the terms are as follows:

- Top EVA layer changes
- Conduction between top EVA and silicon
- Conduction between glass and the top layer of EVA

The conduction between top EVA and silicon can be calculated from the following equations:

$$Q_{\text{cond-PV,EVA1}} = \frac{T_{PV} - T_{EVA1}}{R_{PV,EVA1}} \quad (11)$$

$$R_{PV,EVA1} = \frac{\delta_{PV}}{2k_{PV}A_{PV}} + \frac{\delta_{EVA1}}{2k_{EVA1}A_{EVA1}} \quad (12)$$

Silicon

The energy input to the silicon layer arrives through solar radiation, and the output energy is the product of power generation and heat conduction between the top EVA and silicon and heat conduction between the bottom EVA and silicon, according to

Eq. (13). In the following relation, τ is the transmissivity, and P_{ele} is the production power.

$$c_{p,PV} \delta_{PV} A \rho_{PV} \frac{dT_{PV}}{dt} = \alpha_{PV} \tau_g GA - P_{ele} - Q_{cond-PV,EVA1} - Q_{cond-EVA2,PV} \quad (13)$$

The left-to-right terms in Eq. (13) are

- Silicon layer energy changes
- Solar radiation received by the silicon layer
- Power generation of solar cells
- Conduction between top EVA and silicon
- Conduction between glass and bottom EVA

The conduction between bottom EVA and silicon, as well as the thermal resistance, is calculated from Eqs. (14) and (15):

$$Q_{cond-EVA2,PV} = \frac{T_{PV} - T_{EVA2}}{R_{EVA2,PV}} \quad (14)$$

$$R_{PV,EVA1} = \frac{\delta_{EVA2}}{2k_{EVA2} A_{EVA2}} + \frac{\delta_{PV}}{2k_{PV} A_{PV}} \quad (15)$$

Bottom EVA

The input energy to the bottom EVA layer is the conduction between the bottom EVA and silicon, and the output energy is the conduction between the bottom EVA and Tedlar, which can be calculated according to Eq. (16). The Td subtitle represents the Tedlar layer.

$$c_{p,EVA2} \delta_{EVA2} A \rho_{EVA2} \frac{dT_{EVA2}}{dt} = Q_{cond-EVA2,PV} - Q_{cond-Td,EVA2} \quad (16)$$

The terms of Eq. (16) from left-to-right are

- Energy changes of bottom EVA layer
- Conduction between bottom EVA layer and silicon layers
- Conduction between Tedlar and bottom EVA layers

The conduction between the bottom EVA and silicon and the thermal resistance is calculated from Eqs. (17) and (18).

$$Q_{cond-Td,EVA2} = \frac{T_{EVA2} - T_{Td}}{R_{EVA1,Td}} \quad (17)$$

$$R_{PV,EVA1} = \frac{\delta_{PV}}{2k_{PV}A_{PV}} + \frac{\delta_{EVA1}}{2k_{EVA1}A_{EVA1}} \quad (18)$$

Tedlar

The input energy to the Tedlar layer is through the conductive heat transfer between the bottom EVA layers and the Tedlar, and the output energy is through the transfer of radiative and convective heat between the Tedlar and the ambient air, shown in Eq. (19):

$$c_{p,Td}\delta_{Td}A\rho_{Td}\frac{dT_{Td}}{dt} = Q_{\text{cond-Td,EVA2}} - Q_{\text{conv-Td,a}} - Q_{\text{rad-Td,a}} \quad (19)$$

The terms from left-to-right in Eq. (19) are

- Tedlar layer energy changes
- Conduction between Tedlar and bottom EVA
- Convection between Tedlar and air
- Radiation between Tedlar and surroundings

The method of calculating radiant heat transfer rate and thermal resistance is mentioned in Eqs. (20) and (21):

$$Q_{\text{rad-Td,a}} = \frac{T_{Td} - T_a}{R_{\text{rad-Td,a}}} \quad (20)$$

$$R_{\text{rad-Td,a}} = \frac{1}{\sigma\varepsilon_{Td}A(T_{Td}^2 + T_a^2)(T_{Td} + T_a)} \quad (21)$$

In addition, the convective heat transfer rate between Tedlar layer and air stream is obtained according to Eqs. (22) and (23):

$$Q_{\text{conv-Td,a}} = \frac{T_{Td} - T_a}{R_{\text{conv-Td,a}}} \quad (22)$$

$$R_{\text{rad-Td,a}} = \frac{1}{h_{\text{conv-Td,a}}A} \quad (23)$$

To obtain the convective heat transfer coefficient—which is between the BIPV/T system and the wall of the building—one must consider whether the air channel of the BIPV/T system has forced or free convection. The governing equations for each of these two conditions are introduced in the subsequent part.

The Air Stream Between BIPV/T System and Wall of Building

In this part, first the governing equations for free convection are presented. It follows by presenting the governing equation for forced convection. For both conditions, the heat transfer rate between panel and air ($\dot{Q}_{PV,air}$) can be determined from Eq. (24):

$$\dot{Q}_{PV,air} = \dot{m}_{air} c_{P,air} (T_{air,out} - T_{air,in}) \quad (24)$$

Here, \dot{m}_{air} , $c_{P,air}$, $T_{air,out}$, and $T_{air,in}$ stand for the mass flow rate, isobaric heat capacity, outlet air stream temperature, and inlet air stream temperature, respectively. In addition to Eq. (24), $\dot{Q}_{PV,air}$ can also be defined from Eq. (25):

$$\dot{Q}_{PV,air} = h_{conv-Td,a} A_{PV,air} (T_{Td} - T_{air,mean}) \quad (25)$$

where $A_{PV,air}$ denotes the heat transfer area between PV and air stream. $T_{air,mean}$ is the mean temperature of air stream, which can be considered as the average of the values of inlet and outlet temperature of air stream [24]:

$$T_{air,mean} = \frac{T_{air,out} + T_{air,in}}{2} \quad (26)$$

Free Convection

When the convective heat transfer is free, the convective coefficient can be obtained from Eqs. (27) to (29) [25]:

$$Nu_x = 0.60(\text{Pr} \cdot Gr_x^*)^{1/5} \quad (27)$$

$$Nu_m = 1.25(Nu_x)_{X=L} \quad (28)$$

$$Gr_x^* = Gr_x \cdot Nu_x = \frac{\beta \cdot g \cdot q_w \cdot X^4}{k \cdot \gamma^2}, \quad Nu_x = \frac{X \cdot h_{conv-Td,a}}{k} \quad (29)$$

where X denotes the characteristic length. Moreover, Nu , Pr , Gr , and Gr^* represent the Nusselt number, the Prandtl number, the Grashof number, and the modified Grashof number, respectively. The average Nusselt number is expressed as Nu_m and β , g , q_w , and γ are the temperature constant of the convective coefficient, the acceleration of gravity, the heat flux (energy per unit area) transferred from the wall to the air stream, and the heat capacity ratio (the ratio of isobaric heat capacity to constant volume heat capacity, which is known as the isentropic expansion factor).

Forced Convection

The forced convective heat transfer coefficient between the airflow and the BIPV/T system is given by Eqs. (30) to (32) [24]:

$$h_c = \frac{k}{D_H} \left\{ 0.0182 \text{Re}^{0.8} \text{Pr}^{0.4} \left[1 + j \frac{D_H}{L} \right] \right\} \quad (30)$$

$$j = 14.3 \log \left(\frac{L}{D_H} \right) - 7.9 \quad \text{for } 0 < \frac{L}{D_H} \leq 60 \quad (31)$$

$$j = 17.5 \quad \text{for } \frac{L}{D_H} > 60 \quad (32)$$

where D_H , Re , and L are the hydraulic diameter, Reynolds number, and Length of channel.

The Electrical Model

The primary purpose of PV systems is to generate power, so modeling the electrical power of solar PV systems is very important. There are different ways to predict the electrical performance of PV systems. One of the relations in which the efficiency of the solar system is determined based on the reference conditions is presented in Eq. (33):

$$\eta = \eta_{ref} \left(1 - \beta_{ref} (T_{PV} - T_{ref}) \right) \quad (33)$$

where η_{ref} , β_{ref} , and T_{ref} represent the efficiency, temperature coefficient, and reference temperature. The reference condition for this equation is solar radiation of 800 W.m^{-2} and temperature of $20 \text{ }^\circ\text{C}$, respectively. The reference condition should not be confused with the standard test condition (STC), in which the irradiance and temperature values are 1000 W.m^{-2} and $25 \text{ }^\circ\text{C}$, respectively [26]. These coefficients are provided in the customer catalogs of solar panel manufacturers.

The power of the solar system is calculated by Eq. (34):

$$P_{ele} = \eta_{ref} \left(1 - \beta_{ref} (T_{PV} - T_{ref}) \right) GA \quad (34)$$

Coupling the Two Models

The discussion provided in the previous parts has shown that determining the electrical power requires the PV temperature, and obtaining the PV temperature necessitates knowledge of the electrical power. Therefore, the thermal and electrical stimulation approaches should be coupled together, and the system performance values should be obtained by trial and error. A detailed explanation is available in previous studies by the authors, such as [27]. The trial-and-error process for finding the temperature and electricity production of the system is depicted in Fig. 3.

It is worth mentioning that despite changing the meteorological characteristics by time, by following the same fashion as the published research works in the field such as [28], the equations have been solved in the steady-state condition at each time step. For this purpose, the computer codes developed by a software like MATLAB could be utilized.

Moreover, obtaining the temperature of the outlet air stream is done by following the stages introduced in Fig. 4. As seen, obtaining temperature of PV using the given flowchart of Fig. 3 is a part of that.

Achieving the Net Zero Goal Using BIPV/T Systems

The term “net zero” may refer to two concepts. One is “net zero energy building (NZEB),” referring to a building equipped with renewable energy sources, such as PV panels, to produce the energy required during the year. In cases in which renewable energy sources are not able to meet demand, energy is supplied from the grid. If there is surplus in the generation, the excess is transferred to the network. The net amount of energy transferred from the building to the grid is zero in NZEBs [29]. When referring to NZEBs, the term “net zero” is accompanied by the word “buildings” [30].

The second probable condition the term “net zero” might refer to is “net zero emission (NZE).” Similar to NZEB, NZE means a condition in which the amount of emissions released into the atmosphere is equal to the amount of emissions removed. In order to remove emissions, a variety of solutions can be employed. For instance, CO₂ emissions in the atmosphere can be removed using trees [31].

Using BIPV/T systems can help achieve both NZEB and NZE goals at the same time. The PV panels used in a BIPV/T system represent a type of less fuels like natural gas for heat provision. Moreover, using BIPV/T systems means burning less fossil fuels in furnaces and thermal power plants.

Among related studies, Uygun et al. [32] evaluated the potential of using BIPV systems to achieve NZEB goals in three cities in Turkey: Çanakkale, Antalya, and Rize. The EnergyPlus software program was utilized, while the values of the heating and cooling demand, as well as electricity production, were considered.

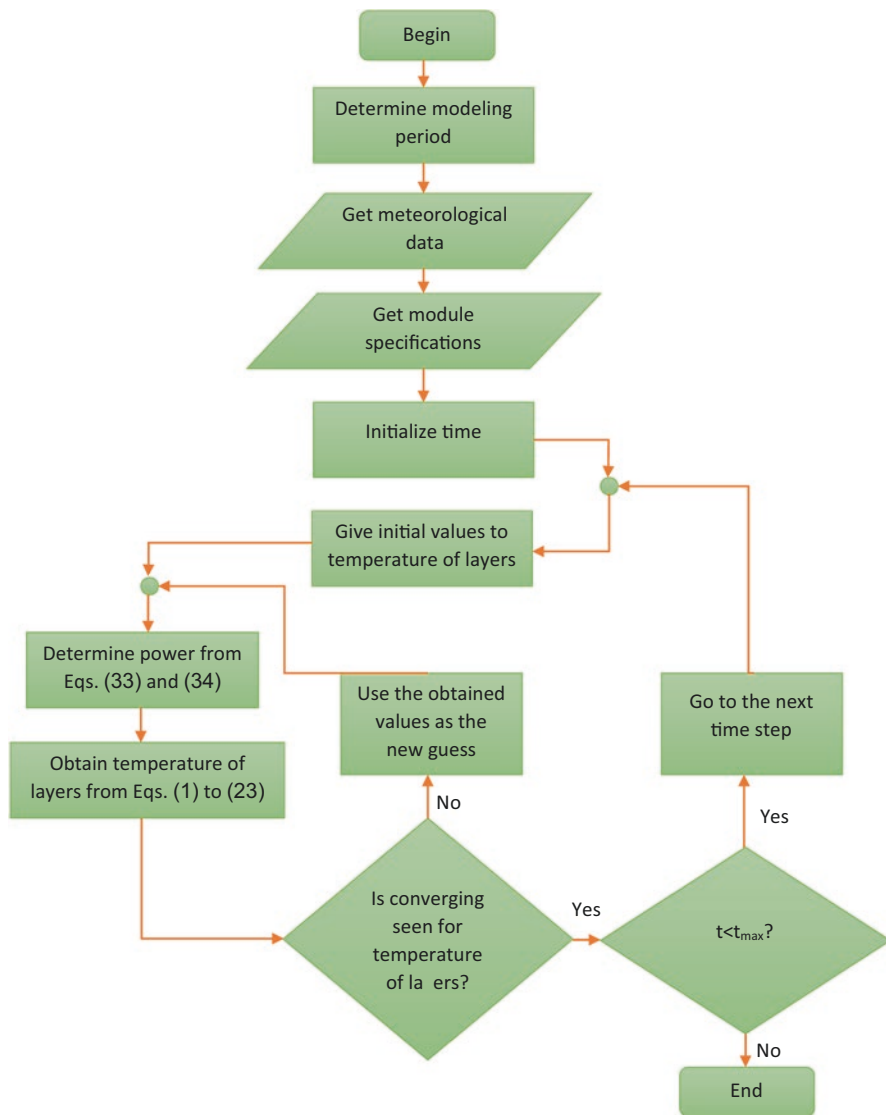


Fig. 3 The trial-and-error process for finding the temperature and electricity production of the system

According to the results, BIPV systems were found to have the potential of meeting the demands for all three locations, which lie in coastal regions.

In another investigation, Nallapaneni and Chopra [33] studied the performance of algal PV for integration with a building face and fulfilling net zero targets. Hong Kong was considered as the case study, and the application in high-rise buildings was investigated. A conceptual design was provided, and a sensitivity analysis was

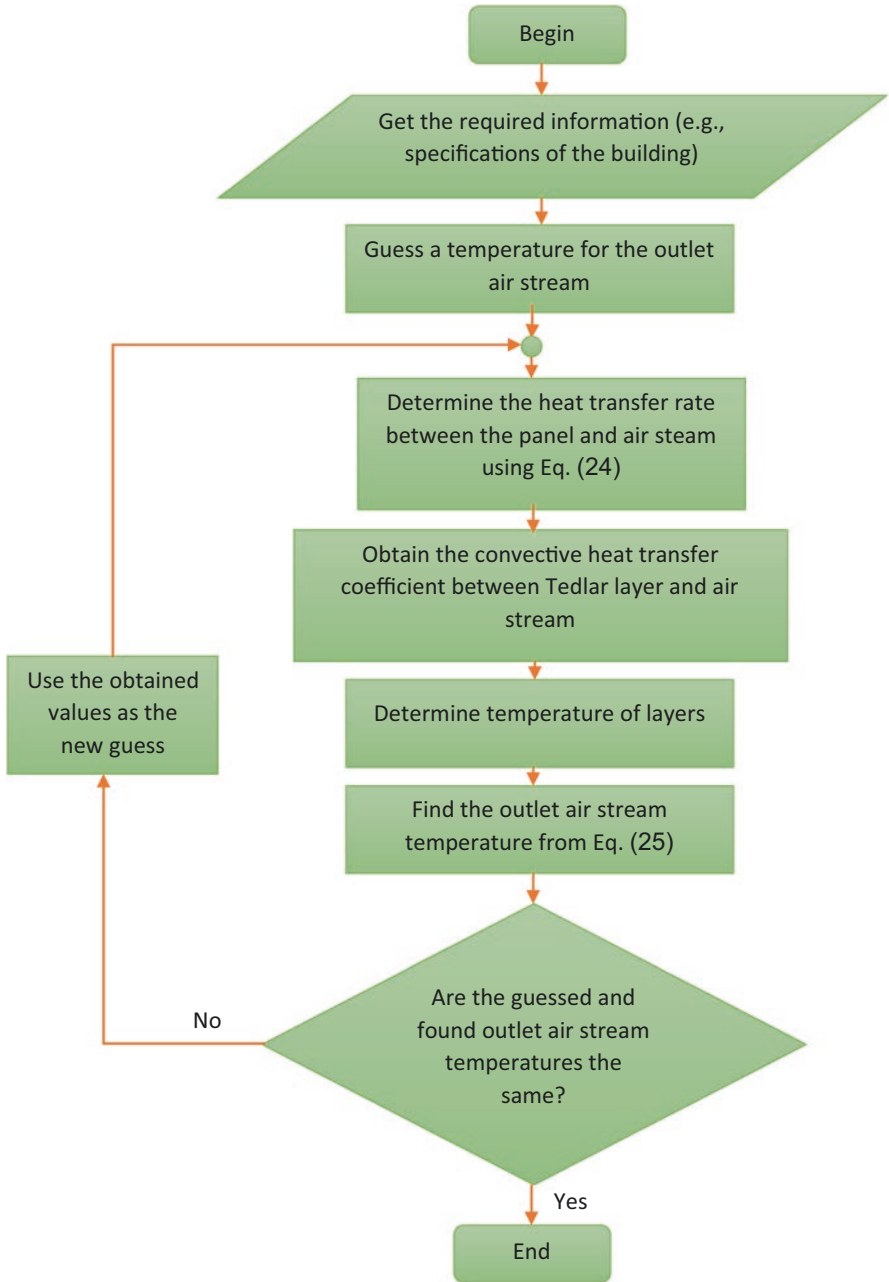


Fig. 4 The trial-and-error process for obtaining the temperature of outlet air stream

conducted to acquire information about the impact of changing solar radiation on system performance. López and Mobiglia [34] chose a heritage building in Switzerland and analyzed the feasibility of employing BIPV systems to reach net zero and positive zero goals.

For a BIPV system in Montreal, Canada, Yip et al. [35] explored the impacts of nine performance criteria, including the shape of the plan, window to wall ratio, and tilt angle. The net energy use intensity in a year was chosen as the system performance indicator. According to the results, the impact of some parameters, such as orientation, was higher than that of others. Another investigation with almost the same research team was conducted in [36].

In addition to the abovementioned studies, in which the net zero concept has been studied directly, a number of other studies have investigated it indirectly. The word indirect refers to investigating the energy and environmental criteria of the system and finding ways for enhancing them, usually by either multi-objective optimization or a parametric study. For instance, Sohani et al. [37] determined the best value of phase change material for integration with a BIPV/T system in Tehran, Iran, by taking a number of objective functions, including environmental and energy ones. The energy generated by the system throughout the year was representative of the energy side, while CO₂ saving was considered by taking the environmental impact into account. A novel optimization method called the dynamic multi-objective optimization approach was employed to gain a better outcome.

Multi-objective optimization was also utilized by Wijeratne et al. [38] with the aim of identifying the best condition for roof sheets and skylights in a BIPV system. The study introduced 7 and 14 solutions for the two aforementioned characteristics, respectively, in the form of non-dominated answers. A passive intelligence concept was proposed by Yoo [5] for a BIPV system, to harvest more irradiance from the sun, as well. According to the paper's discussion, it had a better energy performance, producing more electricity, and was able to reduce the cooling load significantly.

In addition to the research works already mentioned, a number of review studies have also been published during the past years on the topic of achieving net zero goals. Those of Gholami et al. [20], Rosa [39], Awuku et al. [40], Pugsley et al. [41], Ghosh [14], and Wei and Skye [42] can be given as examples.

Conclusion

This work has provided an overview of using both the BIPV and BIPV/T systems to achieve net zero targets. For this purpose, in addition to introducing the BIPV/T concept and the simulation method under both free and forced convection conditions, a number of recent studies have been reviewed in the field of both BIPV and BIPV/T technologies. As noted in our discussion, in a number of research works, sensitivity analysis or a parametric study has been conducted to find the impact of different performance indicators. In another group, different locations have been

considered to identify more suitable places for applying BIPV and BIPV/T technologies. In addition to the indicated groups, there has been one more category in which multi-objective optimization was conducted to acquire the foremost condition for the system decision variables.

According to our discussion, both paths can be recommended for future research. One is to consider both NZEB and NZE targets as suitable for study, with the addition of economic perspectives, like the reduction in levelized cost of energy (LCOE) for renewable energies, to give a broader horizon. Another idea is to employ decision-making tools like AHP, LINMAP, and TOPSIS to consider the priorities of policy-makers and customers and not give the same importance to other performance criteria, which is the current approach studies take.

References

1. Dehghani-Sanij, A. R., & Bahadori, M. N. (2021). *Ice-houses: Energy, architecture, and sustainability*. Elsevier, Imprint by Academic Press.
2. M.R.Khani, S., Bahadori, M. N., Dehghani-Sanij, A. R., & Nourbakhsh, A. (2017). Performance evaluation of a modular design of wind tower with wetted surfaces. *Energies*, 10(7), 845.
3. Dehghani-Sanij, A. R. (2022). Providing thermal comfort for buildings' inhabitants through natural cooling and ventilation systems: Wind towers. In A. Sayigh (Ed.), *Achieving building comfort by natural means*. Springer Nature.
4. Boccalatte, A., Fossa, M., & Ménézo, C. (2020). Best arrangement of BIPV/T surfaces for future NZEB districts while considering urban heat island effects and the reduction of reflected radiation from solar facades. *Renewable Energy*, 160, 686–697.
5. Yoo, S.-H. (2019). Optimization of a BIPV/T system to mitigate greenhouse gas and indoor environment. *Solar Energy*, 188, 875–882.
6. Bauer, A., & Menrad, K. (2019). Standing up for the Paris Agreement: Do global climate targets influence individuals' greenhouse gas emissions? *Environmental Science & Policy*, 99, 72–79.
7. Taveres-Cachat, E., Grynning, S., Thomsen, J., & Selkowitz, S. (2019). Responsive building envelope concepts in zero emission neighborhoods and smart cities—a roadmap to implementation. *Building and Environment*, 149, 446–457.
8. Lancet, T. (2019). Net zero by 2050 in the UK. London, UK. 1911.
9. Hu, M., & Qiu, Y. (2019). A comparison of building energy codes and policies in the USA, Germany, and China: Progress toward the net-zero building goal in three countries. *Clean Technologies and Environmental Policy*, 21(2), 291–305.
10. Ballif, C., Perret-Aebi, L.-E., Lufkin, S., & Rey, E. (2018). Integrated thinking for photovoltaics in buildings. *Nature Energy*, 3(6), 438–442.
11. Jäger-Waldau, A., Kougias, I., Taylor, N., & Thiel, C. (2020). How photovoltaics can contribute to GHG emission reductions of 55% in the EU by 2030. *Renewable and Sustainable Energy Reviews*, 126, 109836.
12. Pierro, M., Perez, R., Perez, M., Moser, D., & Cornaro, C. (2021). Imbalance mitigation strategy via flexible PV ancillary services: The Italian case study. *Renewable Energy*, 179, 1694–1705.
13. Kuhn, T. E., Erban, C., Heinrich, M., Eisenlohr, J., Ensslen, F., & Neuhaus, D. H. (2021). Review of technological design options for building integrated photovoltaics (BIPV/T). *Energy and Buildings*, 231, 110381.

14. Ghosh, A. (2020). Potential of building integrated and attached/applied photovoltaic (BIPV/T/BAPV) for adaptive less energy-hungry building's skin: A comprehensive review. *Journal of Cleaner Production*, 276, 123343.
15. Reddy, P., Gupta, M., Nundy, S., Karthick, A., & Ghosh, A. (2020). Status of BIPV/T and BAPV system for less energy-hungry building in India—A review. *Applied Sciences*, 10(7), 2337.
16. Rounis, E. D., Athienitis, A., & Stathopoulos, T. (2021). Review of air-based PV/T and BIPV/T systems—performance and modelling. *Renewable Energy*, 163, 1729–1753.
17. Debbarma, M., Sudhakar, K., & Baredar, P. (2017). Comparison of BIPV and BIPVT: A review. *Resource-Efficient Technologies*, 3(3), 263–271.
18. Sohani, A., Naderi, S., & Pignatta, G. (2021). 4E advancement of heat recovery during hot seasons for a building integrated photovoltaic thermal (BIPV/T) system. *Environmental Sciences Proceedings*, 12(1).
19. Shakouri, M., Ghadamian, H., Hoseinzadeh, S., & Sohani, A. (2022). Multi-objective 4E analysis for a building integrated photovoltaic thermal double skin Façade system. *Solar Energy*, 233, 408–420.
20. Gholami, H., Nils Røstvik, H., & Steemers, K. (2021). The contribution of building-integrated photovoltaics (BIPV/T) to the concept of nearly zero-energy cities in Europe: Potential and challenges ahead. *Energies*, 14(19), 6015.
21. Cornaro, C., Bartocci, S., Musella, D., Strati, C., Lanuti, A., Mastroianni, S., et al. (2015). Comparative analysis of the outdoor performance of a dye solar cell mini-panel for building integrated photovoltaics applications. *Progress in Photovoltaics: Research and Applications*, 23(2), 215–225.
22. Shahveredian, M. H., Sohani, A., & Sayyaadi, H. (2021). Water-energy nexus performance investigation of water flow cooling as a clean way to enhance the productivity of solar photovoltaic modules. *Journal of Cleaner Production*, 312, 127641.
23. Shahveredian, M. H., Sohani, A., Sayyaadi, H., Samiezadeh, S., Doranehgard, M. H., Karimi, N., et al. (2021). A dynamic multi-objective optimization procedure for water cooling of a photovoltaic module. *Sustainable Energy Technologies and Assessments*, 45, 101111.
24. Shahsavari, A., & Rajabi, Y. (2018). Exergoeconomic and enviroeconomic study of an air based building integrated photovoltaic/thermal (BIPV/T) system. *Energy*, 144, 877–886.
25. Ghadamian, H., Ghadimi, M., Shakouri, M., Moghadasi, M., & Moghadasi, M. (2012). Analytical solution for energy modeling of double skin facades building. *Energy and Buildings*, 50, 158–165.
26. Sohani, A., & Sayyaadi, H. (2020). Providing an accurate method for obtaining the efficiency of a photovoltaic solar module. *Renewable Energy*, 156, 395–406.
27. Sohani, A., Sayyaadi, H., Doranehgard, M. H., Nizetic, S., & Li, L. K. B. (2021). A method for improving the accuracy of numerical simulations of a photovoltaic panel. *Sustainable Energy Technologies and Assessments*, 47, 101433.
28. Gu, W., Ma, T., Shen, L., Li, M., Zhang, Y., & Zhang, W. (2019). Coupled electrical-thermal modelling of photovoltaic modules under dynamic conditions. *Energy*, 188, 116043.
29. The U.S. Department of Energy, Zero Energy Buildings. 2022. <https://www.energy.gov/eere/buildings/zero-energy-buildings>. Accessed on 31 Mar 2022.
30. Abdou, N., El Mghouchi, Y., Hamdaoui, S., El Asri, N., & Mouqallid, M. (2021). Multi-objective optimization of passive energy efficiency measures for net-zero energy building in Morocco. *Building and Environment*, 204, 108141.
31. National Grid ESO, What is net zero and zero carbon?, 2022. <https://www.nationalgrideso.com/future-energy/net-zero-explained/net-zero-zero-carbon>. Accessed on 31 Mar 2022.
32. Uygun, U., Akgül, Ç.M., Dino, İ.G., & Akinoglu, B.G. (2018). Approaching net-zero energy building through utilization of building-integrated photovoltaics for three cities in Turkey—preliminary calculations. In *2018 international conference on photovoltaic science and technologies (PVCon)* (pp. 1–5). IEEE.
33. Nallapaneni, M. K., & Chopra, S. S. (2021). Algal photobioreactor facades coupled with BAPV/BIPV/T in high-rise urban buildings improves indoor air quality and enables energy

- resilience in race to net-zero. In *3rd international conference on renewable energy, sustainable environmental and agricultural technologies*. i-RESEAT.
34. López, C. S. P., & Mobiglia, M. (2021). Swiss case studies examples of solar energy compatible BIPV/T solutions to energy efficiency revamp of historic heritage buildings, In IOP conference series: Earth and environmental science (Vol. 863, No. 1, pp. 012006). IOP Publishing.
 35. Yip, S., Athienitis, A. K., & Lee, B. (2021). Early stage design for an institutional net zero energy archetype building, part 1: Methodology, form and sensitivity analysis. *Solar Energy*, 224, 516–530.
 36. Yip, S., Athienitis, A., & Lee, B. (2019). Sensitivity analysis of building form and BIPV/T energy performance for net-zero energy early-design stage consideration, In IOP conference series: Earth and environmental science (Vol. 238, No. 1, pp. 012065). IOP Publishing.
 37. Sohani, A., Dehnavi, A., Sayyaadi, H., Hoseinzadeh, S., Goodarzi, E., Garcia, D. A., et al. (2022). The real-time dynamic multi-objective optimization of a building integrated photovoltaic thermal (BIPV/T) system enhanced by phase change materials. *Journal of Energy Storage*, 46, 103777.
 38. Wijeratne, W. M. P. U., Samarasinghalage, T. I., Yang, R. J., & Wakefield, R. (2022). Multi-objective optimisation for building integrated photovoltaics (BIPV/T) roof projects in early design phase. *Applied Energy*, 309, 118476.
 39. Rosa, F. (2020). Building-integrated photovoltaics (BIPV/T) in historical buildings: Opportunities and constraints. *Energies*, 13(14), 3628.
 40. Awuku, S. A., Bennadji, A., Muhammad-Sukki, F., & Sellami, N. (2021). A blend of traditional visual symbols in BIPV/T application: Any prospects? *Academia Letters*, 4029.
 41. Pugsley, A., Zacharopoulos, A., Mondol, J. D., & Smyth, M. (2020). BIPV/T facades—A new opportunity for integrated collector-storage solar water heaters? Part 1: State-of-the-art, theory and potential. *Solar Energy*, 207, 317–335.
 42. Wu, W., & Skye, H. M. (2021). Residential net-zero energy buildings: Review and perspective. *Renewable and Sustainable Energy Reviews*, 142, 110859.